

Ab Initio Study of Free-Radical Polymerizations: Cost-Effective Methods to Determine the Reaction Rates

V. Van Speybroeck,^{*,[a]} K. Van Cauter,^[b] B. Coussens,^[c] and M. Waroquier^[d]

The addition of carbon-centered radicals to ethene, which are important in free-radical polymerization processes, are studied from a theoretical point of view. Experimental data for the rate constants are only available for the addition of methyl, ethyl, propyl and butyl radicals. The latter reactions are taken as model systems to derive a cost-effective method for the addition of alkyl radicals to ethene. The proposed model must be accurate and computationally feasible for additions in which larger radicals

are involved. Accuracy is validated by direct comparison of theoretical and experimental rate constants in the temperature range from 300 to 600 K. A variety of electronic-structure methods were tested ranging from Hartree-Fock and post-Hartree-Fock methods to pure and hybrid density functional theory methods. Molecular partition functions were refined by treating large amplitude vibrations beyond the harmonic oscillator approximation.

1. Introduction

Free-radical polymerization is an important and well-established process for the production of polyethylene. Initiation and propagation take place by the addition of radicals to vinylic compounds such as ethylene. A profound knowledge of the factors that determine the rate of these addition reactions is of crucial importance to establish a realistic kinetic model of the chemical process. This can lead to a better insight and optimization of the current production process. For some monomers, for example, styrene, the experimental determination of the propagation rate constant (k_p) is relatively easy, but for other systems, such as acrylates, a cumulation of experimental obstacles hinders the measurement.^[1,2] A major cause of this problem is the fact that several reactions, for example, propagation, transfer, and termination, are taking place simultaneously and that the interpretation of experimental kinetic data is model-dependent.

However, due to advanced experimental techniques (e.g., pulsed-laser techniques), the quality by which rate-coefficients of propagation and termination in free-radical polymerizations may be measured, has substantially improved. Within this respect we refer to the review by Beuermann and Buback.^[3] Still it remains difficult to assess the rate-coefficients of elementary reaction steps, which may be important when determining the chain-length dependence of the propagation rate coefficient. In this field theoretical calculations on the reaction rates can contribute substantially to a better interpretation of the experimental data and even predict effects which are not accessible from an experimental point of view.

Herein, free-radical polymerization of ethene is chosen as a model system. The reactions of interest concern the addition of carbon-centered radicals to ethene and are of intrinsic interest within both polymerization and combustion chemistry. Despite their relevance only a small amount of experimental data are available on a limited set of reactions, namely the addition of methyl, ethyl, propyl and butyl radicals to ethene.^[4-8]

Nevertheless a lot of theoretical investigations have been reported in literature concerning the addition of carbon-centered radicals to vinylic compounds.^[9] The review by Fischer and Radom is very instructive since it gives an overview of the factors controlling the addition of carbon-centered radicals to ethene.^[10] We also note the work of Heuts et al. on the determination of Arrhenius parameters for similar free-radical polymerizations.^[11,12] In these studies, calculations on an extensive level of theory were also performed, but the authors only compared Arrhenius parameters at a given temperature with theoretical predictions. No direct comparison was made between the theoretical and experimental reaction rates in the temperature interval of interest.


The principal aim herein is to determine a cost effective theoretical model to calculate the rates of radical addition to olefins. The final model must be accurate but also computationally feasible, not only for the lower additions but also for those in which larger alkyl radicals are involved. The accuracy of the various theoretical methods must by preference be validated by comparing directly experimental and theoretical rate constants in the relevant temperature range. This criterion is more

[a] Dr. V. Van Speybroeck
Laboratory of Theoretical Physics, Ghent University
Proeftuinstraat 86, 9000 Ghent (Belgium)
Fax: (+32) 9-264-6560
E-mail: veronique.vanspeybroeck@ugent.be

[b] K. Van Cauter
Laboratory of Theoretical Physics, Ghent University
Proeftuinstraat 86, 9000 Ghent (Belgium)

[c] Dr. B. Coussens
DSM Research Department, PO Box 18, 6160 MD Geleen (The Netherlands)

[d] Prof. Dr. M. Waroquier
Laboratory of Theoretical Physics, Ghent University
Proeftuinstraat 86, 9000 Ghent (Belgium)

 Supporting information for this article is available on the WWW under <http://www.chemphyschem.org> or from the author.

reliable than assessments based on kinetic parameters, deduced from the Arrhenius rate law, such as the activation energy and the frequency factor. The strong correlation between both quantities makes a reliable determination of them rather questionable.

Various reaction rate theories are available, strongly varying in computational cost. Among these, transition state theory is one of the oldest but probably the most widely used, due to its relative simplicity.^[13–17] The rate constant is given in Equation (1), where k_B represents Boltzmann's constant, T stands for the absolute temperature, h is Planck's constant and V is the reference volume in which the translational part of the partition function is evaluated.

$$k(T) = \frac{k_B T}{h} \frac{(q_{\ddagger}/V)}{(q_A/V)(q_B/V)} e^{-\frac{\Delta E_0}{k_B T}} \quad (1)$$

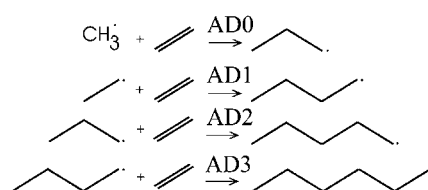
The molecular partition functions q_A and q_B relate to the two reactants and q_{\ddagger} stands for the molecular partition function of the transition state. ΔE_0 represents the molecular energy difference at absolute zero between the activated complex and the reactants, with inclusion of the zero point vibrational energies. $k(T)$ does not depend on the complete potential energy surface, but only on the properties of the transition state and the reactants.

The barrier height depends predominantly on the method used for the electronic structure calculations. A particular difficulty is encountered here since the systems of interest are open shell systems with an odd number of electrons. For such systems the unrestricted Hartree–Fock (UHF) method has been widely used although it has been recognized for many years that UHF methods systematically over-estimate the barrier heights.^[18] Attempts to improve the UHF wavefunctions by many-body perturbation theory, as is done in the popular unrestricted Møller–Plesset second-order method (UMP2), is not as successful as for closed-shell systems since the UHF wavefunction does not provide a suitable reference state for the perturbation theory treatment due to the occurrence of spin contamination.^[19,20] A method to circumvent the problems of spin contamination at transition states is to use a multi-configuration self-consistent-field (MCSCF) wavefunction as reference state for a treatment of dynamical correlation energy.^[21] Unfortunately, all mentioned post-Hartree–Fock methods are computationally very intensive and only applicable to relatively small systems. They do not provide a viable alternative for addition reactions in which longer alkyl radicals are involved. Hybrid Hartree–Fock density functional theory (hybrid DFT) is of great interest for computational thermochemistry and kinetics. Its low computational cost makes it a very attractive alternative for many applications. There are several varieties of hybrid DFT based on various mixing fractions and functionals.^[22] More recent density functionals show great promise in improving the calculation of reaction barrier heights and transition-state geometries.^[23]

The frequency factor is determined by the model in which the molecular partition function is evaluated. For the nuclear motion, one commonly uses the harmonic oscillator (HO) ap-

proximation. This may be adequate for some molecules at low temperatures as long as the system remains in the part of the potential energy surface where the harmonic oscillator approximation to the potential energy surface holds. Many molecules contain “large amplitude” or “low frequency motions” that are characterized by strongly anharmonic potentials. Examples are internal rotations, inversions, and quartic oscillations.^[24,25,26] Hindered rotations are the most known and have been widely studied in one dimension, when the potential can be expressed as a sum of single Fourier terms. It has been shown that such a simplified one-dimensional model with asymmetric internal rotors can improve the result of the reaction rate substantially.^[27]

Herein, we use a variety of post-Hartree–Fock methods and DFT based methods on the first four addition reactions for which experimental rate constants in the gas phase are known (as schematically shown in Scheme 1). The theoretical method



Scheme 1. Reaction Scheme for the studied radical-addition reactions.

must fulfill specific criteria to be retained for further addition reactions in which larger radicals are involved. These criteria are based both on computational grounds, that is, how expensive is the method, and on accuracy. Only methods in good agreement with the experimental rate constants in the relevant temperature regime are retained. The problem of internal rotations and its impact on the reaction rate is also addressed. These intensive comparative studies with experimental data will reveal a theoretical method that is cost effective for calculating rates of free-radical polymerizations. We do however want to stress that it is not the aim to propose a method that is suitable for all possible additions to olefins. Extensive studies on such items, that is, where triple bonds are also involved or hetero-elements C=S bonds have been performed by Radom and co-workers and we refer to these works for more elaborate discussions.^[29,30] Reactions in which longer alkyl radicals are involved will be treated in a subsequent paper, that focusses on the chain-length dependence on the rate coefficients. It may be expected that modifications to the model will be necessary since the longer alkyl radicals occur in the liquid or condensed phase.

Computational Section

Calculations were carried out using Gaussian 98 software and in all cases we adopt the nomenclature for a method as indicated in this program.^[31]

Electronic structure methods: In this paragraph a brief overview is given of all electronic structure methods used in this paper. It is

not the intention of the authors to review the theoretical background of these methods but for the transparency of the paper the notations are introduced which will be used throughout the rest of the paper.

A series of Hartree–Fock and post-Hartree–Fock based methods are applied that are based on unrestricted Hartree–Fock theory (UHF), unrestricted Møller–Plesset second-order and fourth-order theory (UMP2, UMP4), unrestricted quadratic configuration interaction theory with single and double excitations (UQCISD), unrestricted coupled-cluster theory with single and double excitations that also include a quasi-perturbative treatment of fourth- and fifth-order-connected triple-excitation terms (UCCSD(T)).^[18, 19, 28, 32, 33] Additionally, a series of DFT based methods were applied. For the BP86 and BLYP functionals, gradient corrections have been introduced using the Becke exchange part (B) and either the Perdew (P86) or the Lee, Yang and Parr (LYP) correlation parts.^[34, 35, 36] The latter functionals are pure DFT models. Hybrid Hartree–Fock densityfunctional theory (hereafter called hybrid DFT) is set up by mixing various amounts of the Hartree–Fock (HF) nonlocal exchange operator with DFT exchange correlation functionals. Very promising hybrid functionals are B3LYP, B3PW91 and mPW1PW91.^[37, 38] These hybrid DFT methods have proven to be successful for obtaining accurate molecular structures, vibrational frequencies and bond energies.^[39] The most important parameter that varies in these methods is the fraction of HF exchange, set to 20% in B3LYP and B3PW91 and 25% in mPW1PW91. The latter uses the modified Perdew Wang exchange functional that has improved the long-range behavior as proposed by Adamo and Barone.^[38] Other hybrid functionals used in this paper are BHandH and BHandHLYP which further vary by the amount of exact Hartree–Fock exchange that is taken into account and the explicit form for the correlation functional which in this case is given by the LYP functional.^[36, 40] Finally, the recent hybrid functional MPW1K proposed by Truhlar and co-workers was tested.^[41] This modified Perdew–Wang one-parameter model for kinetics was optimized against a database of 20 forward barrier heights, 20 reverse barrier heights and 20 twenty energies of reactions. This functional is used with the 6-31+G(d,p) basis as is recommended in the original paper.^[41]

Computational Details: All stationary points were located and characterized by full geometry optimizations. When possible, analytical computations of the force constants and vibrational frequencies were performed. In the MP4 and QCISD computations the first derivatives were obtained analytically whereas single numerical differentiation was applied to obtain the second derivatives. At the CCSD level only energies are available and therefore a double numerical differentiation is applied.

The influence of basis sets on the results was tested by performing all calculations with the double zeta 6-31G and triple zeta 6-311g basis where extra-polarization functions were also added leading to the 6-31G(d) and 6-311G** basis sets. Basis set saturation was further investigated for the B3LYP model by using more extended 6-31+G(d) and 6-311++G(3df,2p) basis, in which diffuse functions were also added. A recent article by Truhlar and co-workers highlights the effectiveness of diffuse basis functions for the calculation of relative energies by DFT.^[42]

2. Results and Discussion

2.1 Reaction Scheme

The reactions studied are shown schematically in Scheme 1 where the n th addition reaction is labeled as AD n (AD n = C $_{n+1}$ H $_{2n+3}$ + C $_2$ H $_4$ → C $_{n+3}$ H $_{2n+7}$). The product of the n th addition

reaction corresponds to the reactant of the ($n+2$)th reaction since the carbon atoms are added in pairs. In this way the sequences AD1-AD3-AD5-... and AD2-AD4-AD6-... model the propagation phase of the polymerization process.

The first reaction AD0 is in principle an initiation reaction of the methyl radical to the monomer unit, in this case ethene. All following reactions are propagation reactions: AD1 corresponds with the addition of the ethyl radical to ethene, resulting in the butyl radical. A second addition of ethene leads to the production of a hexyl radical (reaction AD3).

Herein, we only discuss reactions AD0, AD1, AD2 and AD3 for which experimental kinetic data are available in the gas phase. In a forthcoming paper of this series we discuss further addition reactions to study the influence of the chain length on the rate constant. Herein, the most suitable and accurate level of theory emerging from the present paper will be used, although modifications will be needed to account for the effects of the liquid or condensed phase. The electronic structure methods must be of intrinsic quality for the chosen addition reactions but the theoretical schemes to treat the internal motions will need further extensions.

2.2 Rate Curves for AD0, AD1, AD2 and AD3

2.2.1 AD1 Reaction

Experimental data are available in five literature works, but only the rate expression proposed by Knyazev and Slagle covers the full temperature range and we will therefore focus on their results.^[5] The other experimental data are similar but measured in more restricted temperature intervals.

The validity and accuracy of a theoretical model for the prediction of the kinetics of a reaction, is based upon the reproduction of the whole rate curve (lnk versus 1/T) in the relevant temperature range rather than deducing the activation energy and pre-exponential factor from the Arrhenius rate law. These quantities can vary to a large extent depending on the temperature range in which they have been adjusted. In order to get a suitable tool for a serious comparative study between various theoretical results we constructed a grid covering the full temperature range. In each interval between two grid-points we determine the preexponential factor and activation energy by means of a least square fitting procedure. The activation energy is given by the slope of the rate curve, while the preexponential factor is derived from the intercept of the curve for 1/T → 0. This procedure is applied for the experimental and for all theoretical predictions of the rate curve. For each chosen small (10 K) temperature interval, the discrepancy with the experiment is determined. The results are summarized in Table 1. The largest deviation of the activation energies is maintained and reported in the first row of the results belonging to each level of theory (see Table 1). These errors may vary from -20 kJ mol⁻¹ to +40 kJ mol⁻¹. We propose as a first “model criterion” a tolerance of 10% deviation on the slope or activation energy from the experiment. Following levels meet this criterion I: BLYP/6-31G(d), BLYP/6-311G(d,p), B3LYP/6-31G(d), MPW1PW91/6-31G(d), MPW1PW91/6-31+G(d), MPW-

Table 1. Error analysis on reaction rate for AD1.

	BP86 6-31G(d)	BP86 6-311G(d,p)	BLYP 6-31G(d)	BLYP 6-311G(d,p)	B3LYP 6-31G(d)	B3LYP 6-31+G(d)	B3LYP 6-311G(d,p)	B3LYP 6-311++G(3df,2p)	MPW1PW91 6-31+G(d)	
	Maximum error on slope in temperature range 300–600 K									
[a]	−7.95	−4.69	−2.72	2.90	2.33	8.05	7.42	10.69	−1.92	
[b]	27.33	16.10	9.14	9.21	7.61	27.32	25.10	36.34	−6.38	
	Error analysis on k									
T										
300	3.86E+01	7.80E+00	2.89E+00	2.69E−01	3.09E−01	2.60E−02	3.32E−02	8.04E−03	1.79E+00	
350	2.45E+01	5.97E+00	2.48E+00	3.14E−01	3.51E−01	4.09E−02	5.04E−02	1.47E−02	1.61E+00	
400	1.74E+01	4.88E+00	2.21E+00	3.51E−01	3.84E−01	5.73E−02	6.86E−02	2.30E−02	1.48E+00	
450	1.34E+01	4.18E+00	2.02E+00	3.83E−01	4.12E−01	7.43E−02	8.72E−02	3.27E−02	1.39E+00	
500	1.09E+01	3.70E+00	1.88E+00	4.11E−01	4.36E−01	9.17E−02	1.06E−01	4.32E−02	1.32E+00	
550	9.17E+00	3.35E+00	1.78E+00	4.37E−01	4.58E−01	1.09E−01	1.24E−01	5.45E−02	1.27E+00	
600	7.99E+00	3.10E+00	1.70E+00	4.61E−01	4.78E−01	1.26E−01	1.42E−01	6.62E−02	1.24E+00	
$\langle f_k \rangle$	1.64E+01	4.59E+00	2.11E+00	3.77E−01	4.06E−01	7.49E−02	8.72E−02	3.42E−02	1.43E+00	
	MPW1PW91 6-31G(d)	MPW1PW91 6-311G(d,p)	BHandH 6-31G(d)	BHandH 6-311G(d,p)	BHandHLYP 6-31G(d)	BHandHLYP 6-311G(d,p)	B3PW91 6-31G(d)	B3PW91 6-311G(d,p)	MPW1K 6-31+G(d,p)	
	Maximum error on slope in temperature range 300–600 K									
[a]	3.07	2.12	−19.54	−15.75	7.99	13.53	1.94	5.62	4.93	
[b]	10.88	6.53	−67.17	−54.09	27.28	46.37	5.99	18.61	16.46	
	Error analysis on k									
T										
300	2.24E−01	3.41E−01	2.82E+03	4.79E+02	2.39E−02	2.19E−03	4.57E−01	8.69E−02	7.97E−02	
350	2.68E−01	3.81E−01	9.25E+02	1.95E+02	3.77E−02	4.73E−03	5.05E−01	1.18E−01	1.05E−01	
400	3.05E−01	4.12E−01	4.00E+02	9.90E+01	5.27E−02	8.39E−03	5.42E−01	1.49E−01	1.28E−01	
450	3.39E−01	4.38E−01	2.08E+02	5.86E+01	6.83E−02	1.31E−02	5.73E−01	1.78E−01	1.50E−01	
500	3.69E−01	4.60E−01	1.24E+02	3.85E+01	8.41E−02	1.87E−02	6.00E−01	2.05E−01	1.70E−01	
550	3.96E−01	4.81E−01	8.12E+01	2.74E+01	9.99E−02	2.51E−02	6.25E−01	2.32E−01	1.89E−01	
600	4.21E−01	5.00E−01	5.72E+01	2.07E+01	1.16E−01	3.21E−02	6.47E−01	2.57E−01	2.07E−01	
$\langle f_k \rangle$	3.33E−01	4.32E−01	5.14E+02	1.10E+02	6.87E−02	1.45E−02	5.66E−01	1.76E−01	1.47E−01	
	UHF 3-21G(d)	UHF 6-31G(d)	MP2 6-31G(d)	MP2 6-311G(d,p)	MP4 6-31G(d)	MP4 6-311G(d,p) ^[c]	qcisd 6-31G(d)	qcisd 6-311G(d,p)	ccsd(t) 6-31G(d)	ccsd(t) 6-311G(d,p) ^[c]
	Maximum error on slope in temperature range 300–600 K									
[a]	8.02	20.77	40.02	34.69	34.47	27.34	16.77	13.53	13.98	8.51
[b]	26.53	70.43	134.61	119.56	118.81	93.80	57.81	46.63	48.17	28.89
	Error analysis on k									
T										
300	1.81E−02	1.33E−04	9.08E−08	4.46E−07	3.96E−07	1.37E−05	6.23E−04	2.74E−03	2.40E−03	2.60E−02
350	2.82E−02	4.27E−04	8.51E−07	3.25E−06	2.85E−06	6.50E−05	1.63E−03	5.94E−03	5.35E−03	4.20E−02
400	3.91E−02	1.02E−03	4.56E−06	1.43E−05	1.24E−05	2.09E−04	3.33E−03	1.06E−02	9.70E−03	6.00E−02
450	5.04E−02	2.02E−03	1.69E−05	4.51E−05	3.88E−05	5.16E−04	5.79E−03	1.65E−02	1.54E−02	7.91E−02
500	6.19E−02	3.49E−03	4.84E−05	1.13E−04	9.63E−05	1.07E−03	9.02E−03	2.36E−02	2.22E−02	9.88E−02
550	7.35E−02	5.48E−03	1.15E−04	2.38E−04	2.03E−04	1.93E−03	1.30E−02	3.16E−02	3.00E−02	1.19E−01
600	8.50E−02	8.01E−03	2.39E−04	4.45E−04	3.77E−04	3.18E−03	1.76E−02	4.05E−02	3.87E−02	1.39E−01
$\langle f_k \rangle$	5.08E−02	2.76E−03	5.11E−05	1.07E−04	9.07E−05	9.01E−04	6.99E−03	1.83E−02	1.72E−02	8.02E−02

[a] Maximum absolute error on slope in the temperature interval 300–600 K. [b] Maximum relative error, expressed in percent, in the temperature interval. [c] Geometries and frequencies were taken from the B3LYP/6-31G(d) level, while the energies were calculated at the current level.

1PW91/6-311G(d,p), and B3PW91/6-31G(d). This criterion is equivalent with a maximum discrepancy of $\approx 3 \text{ kJ mol}^{-1}$ for the activation energy in the whole temperature range and is reflected in the slope of the rate curves. We do however want to point out that the first selection criterion is very strict. The final evaluation or rejection of a computational strategy is however based on two independent criteria of which the second is based on the correspondence between the experi-

mental and theoretical rate constant. Figure 1a displays the theoretical rate curves that fulfill criterion I as well as the experimental curve. Another aspect is the shift of the rate curve with respect to the experimental one, which reflects the deviation from the experimental pre-exponential factor and which will be the major selection parameter in criterion II.

To quantify the deviation of the theoretical rate constant with respect to the experimental value, we introduced a factor

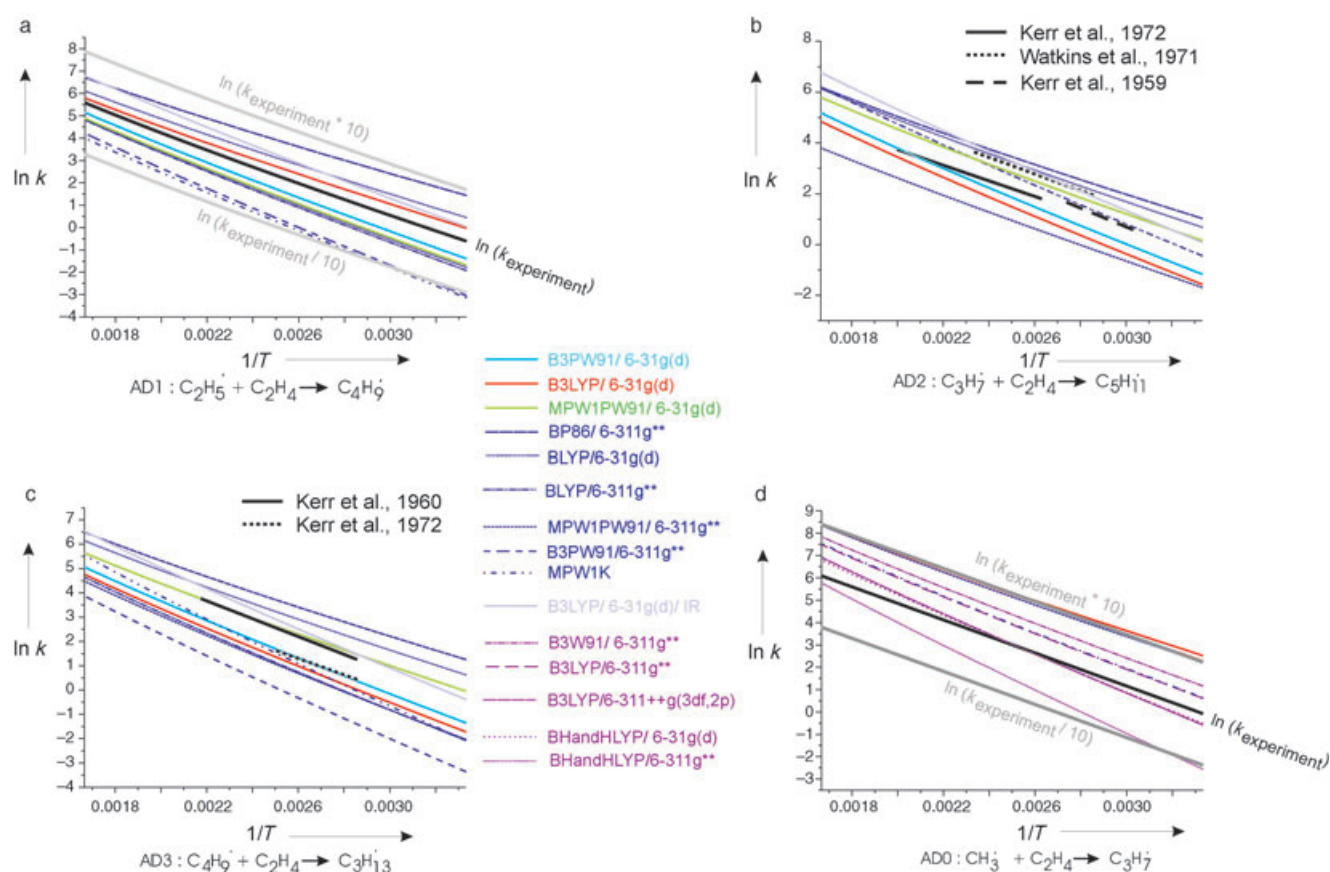


Figure 1. a)–d) Rate curves of $\ln k$ versus $1/T$ for the reactions AD1, AD2, AD3 and AD0, respectively. Only the theoretical methods that fulfill criteria I or II are taken up. The rate k is expressed in units $\text{m}^3 \text{mol}^{-1} \text{s}^{-1}$.

$f_k = k_{\text{theory}}/k_{\text{experiment}}$. This quantity is given in Table 1 at various temperatures together with the average value of f_k in the interval from 300–600 K. All theoretical methods that fulfill criterion I, deviate at maximum a factor of three with the experimental rate constant.

The ratio f_k is determined both by the slope of the rate curve but also by the shift relative to the experimental one and thus it also comprises effects of the pre-exponential factor. This means that the ratio f_k is also determined by the method used to construct the molecular partition functions. In the simplest approximation this is done by factorizing the latter quantity into an electronic, rotational, translational and internal motion fraction. The factorization of the global rotational and internal motion is not correct but this coupling is generally neglected. The internal motions are furthermore treated in the HO approximation, taking only small deviations from the reference conformer into account. This model is known to be inaccurate for modeling kinetic and thermodynamic quantities of molecular species and large errors can be introduced into the partition function.^[43] Various theoretical schemes have been introduced to go beyond the HO approximation. One of the simplest is the internal rotor approximation (IR) in which all internal rotations are decoupled and taken into account by determining the rotational energy levels in the one-dimensional rotational potential. More theoretical details can be found in refs. [27,45].

To estimate the magnitude of the corrections due to internal rotations, we have taken into account uncoupled internal rotations for the AD1 reaction at the B3LYP/6-31G(d) level of theory. Only three internal rotations are present: the methylene rotation-inversion in the ethyl radical (ER), the rotation of the approaching ethyl radical about the forming C–C bond in the transition state and the methyl rotation in the transition state (TSBR). The rotational potentials for these torsions are shown in Figure 2. We are not going into detail into the properties of these potentials since an elaborate discussion was already given in ref. [27] on a similar addition reaction, that is, the addition of the ethylbenzene radical to ethene. We only mention the appearance of an additional transition state corresponding to the gauche attack of the ethyl radical to ethene which is energetically favored by 0.7 kJ mol^{-1} . The partition function of the transition state in the IR approach increases by approximately a factor of four compared to the HO model. This enhancement can be understood since more conformers and thus more transition states come into play. For a detailed discussion we refer to ref. [27]. The methylene rotation in the ethyl radical is characterized by extremely low barriers (0.3 kJ mol^{-1}) and is treated in the free rotor model. The partition function of this radical decreases by about a factor of two in the latter model. The decrease can mainly be attributed to the inclusion of a symmetry number of six in the internal rotor model. Replacing the HO partition functions by the IR esti-

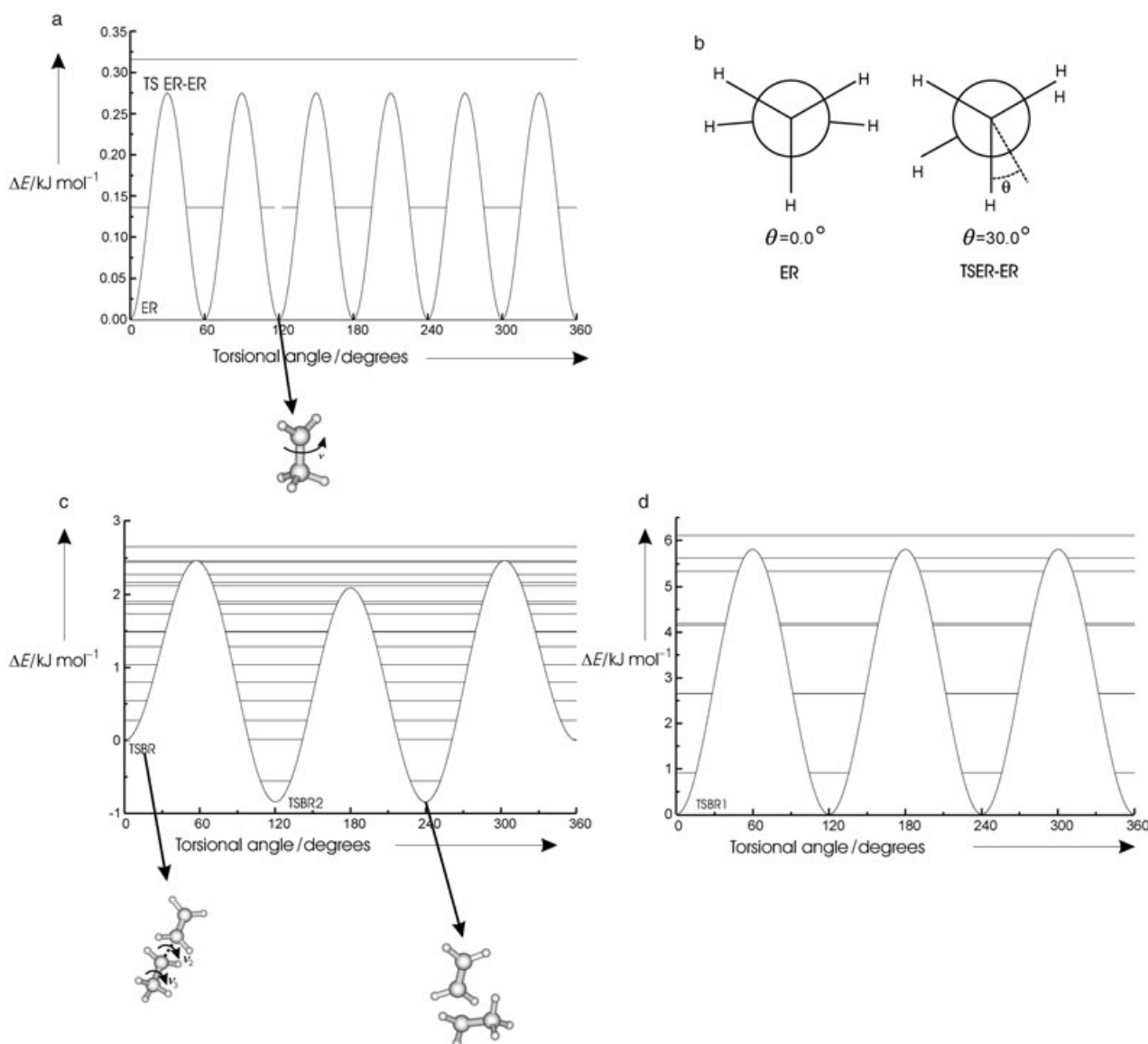


Figure 2. a) Rotational potential for the methylene rotation in the ethyl radical, b) Newman projections for the stationary points of the methylene rotation in the ethyl radical, c) and d) Rotational potentials for the ethylene and methyl rotation in the transition state for reaction AD1. All potentials are obtained at the B3LYP/6-311G(d,p) level of theory.

mates increases the reaction rate by approximately a factor of seven. The enhancement due to the IR corrections is in the same order of magnitude for all levels of theory. The methods that underestimate the rate in the HO model, that is, BLYP/6-311G(d,p), B3LYP/6-31G(d), B3PW91/6-31G(d), and MPW1PW91/6-311G(d,p), will overestimate the rate (by approximately a factor of three) in the IR model but still fall within the acceptable range to retain the theoretical method. The methods BLYP/6-31G(d) and MPW1PW91/6-31G(d) overestimate the rate in the IR model by about a factor 10 to 15. For further discussion a criterion II is proposed to retain a theoretical method, corresponding to a maximum deviation of the ratio f_k by a factor of ten in the whole temperature range.

Figure 1a shows the theoretical rate constants that fulfill either criteria I or II together with the empirical values in the relevant temperature range, that is, 300–600 K. Also the

B3LYP/6-31G* rate curve with inclusion of internal rotations is shown. The latter extension mainly induces a shift of the rate curve towards higher values, without substantially altering the activation energies.

Based on criterion I, that is, the activation energy may at maximum deviate 3 kJ mol^{-1} over the whole temperature range corresponding to a deviation of 10%, the methods BLYP/6-31G(d), BLYP/6-311G(d,p), B3LYP/6-31G(d), MPW1PW91/6-31G(d), MPW1PW91/6-311G(d,p), and B3PW91/6-31G(d) can be retained. For all these methods the rate constants deviate at maximum with a factor of three within the HO model. If internal rotations are taken into account, the levels of theory BLYP/6-311G(d,p), B3LYP/6-31G(d), B3PW91/6-31G(d), and MPW1PW91/6-311G(d,p) agree closer with the experimental value, while the other two selected methods MPW1PW91/6-311G(d,p), and B3PW91/6-31G(d), which satisfy criterion I, fail

and predict reaction rates differing at least by a factor of ten from the experimental values.

2.2.2 AD2 Reaction

For AD2 three experiments are available but none of them covers the full temperature range (300–600 K).^[6] Moreover the slope of the Arrhenius plots varies substantially, that is, from 25.5 to 31.0 kJ mol⁻¹, among the various experiments. Therefore it is difficult to reject or retain a theoretical method solely on the degree of correspondence with the slope of the experimental rate curve. It is better to focus on the error analysis resulting from direct comparison of experimental and theoretical rate constants. The error analysis on the reaction rate of AD2 is taken up in table S.1 of the supporting information.

When retaining only those methods that fulfill criterion II, the following electronic structure methods can be retained: BP86/6-311G(d,p), BLYP/6-31G(d), BLYP/6-311G(d,p), B3LYP/6-31G(d), MPW1PW91/6-31G(d), MPW1PW91/6-311G(d,p), and B3PW91/6-31G(d). These levels satisfy the criterion for all three experiments. The resulting rate curves for these selected methods together with the experimental data are visualized in Figure 1b. Taking into account internal rotations in the uncoupled scheme, the reaction rate is enhanced by approximately a factor of six and brings the B3LYP/6-31G(d) curve closer to the experimental rate constant.

2.2.3 AD3 Reaction

The experiments available for this reaction are quite limited and only available in the temperature range from 350 to 450 K.^[7] Given the experimental error bars, we focus on the rate constants themselves for selecting appropriate levels of theory. The error analysis on the reaction rate of AD2 is taken up in table S.2 of the supporting information. The following methods show deviations of less than a factor ten with the experimental rate constants: BP86/6-311G(d,p), BLYP/6-31G(d), BLYP/6-311G(d,p), B3LYP/6-31G(d), MPW1PW91/6-31G(d), MPW1PW91/6-311G(d,p), B3PW91/6-31G(d), and MPW1K. The influence of internal rotations on this reaction contributes with about a factor of five to the global rate constant. The resulting rate curves are shown in Figure 1c.

2.2.4 AD0 Reaction

This reaction is in principle an initiation reaction, but is included in the discussion for completeness. There are six experiments available in the gas phase, of which five of them give rates in the relevant temperature range, that is, 300–600 K.^[4] We will base our discussion on the experiments of Baulch et al. and Tsang et al. since they cover the full temperature range. The activation energies of these experiments differ slightly (ranging from 30.8 kJ mol⁻¹ to 32.3 kJ mol⁻¹). The error analysis on the reaction rate of AD0 is taken up in table S.3 of the supporting information. Based on criterion I, the following methods result: B3LYP/6-31G(d), MPW1PW91/6-311G(d,p), and B3PW91/6-31G(d). Based on criterion II, the following addition-

al methods can be retained B3LYP/6-311G(d,p), B3LYP/6-311+g(3df,2p), MPW1PW91/6-311G(d,p), BHandHLYP/6-31G(d), BHandHLYP/6-311G(d,p), B3PW91/6-311G(d,p), and MPW1K. Only the B3LYP/6-31G(d) and MPW1PW91/6-311G(d,p) methods fulfill both selection criteria. The influence of internal rotations is much smaller for this reaction, that is, $k_{\text{IR}}/k_{\text{HO}}$ varies around one, which is not surprising since no additional conformers of the transition-state or reactants come into play in the IR model.

2.3 General Remarks and Selection of Cost-Effective Theoretical Models

In this section we summarize the results for the various radical reactions in order to propose theoretical models that are cost-effective, in the sense that they are computationally feasible and accurate.

Figure 3 gives a schematic overview of the error analysis on the theoretical rate constant with respect to the experimental value for each method. As discussed before, the selection of the most suitable level of theory is based on the reproduction of the correct slope for the rate curve (criterion I) or on the reproduction of rate constants within a factor of ten (criterion II). The factor f_k gives an indication for the error on the predicted rate constant. Criterion I was not used for the reactions AD2 and AD3 since the errors on the experimental activation energies are too large (about 5 kJ mol⁻¹). The final selection of methods will be primarily based on the reactions AD1, AD2 and AD3 since they are representative for further propagation reactions while AD0 is in principle an initiation reaction.

To give an idea of the possible influence of taking into account internal rotations more profoundly, a factor $f_{\text{IR}} = k_{\text{theory,IR}}/k_{\text{theory,HO}}$ is introduced. It reflects the increase or decrease of the rate constant in the Internal Rotor approximation with respect to the standard HO model. This quantity gives only a rough indication, as various models can be used to treat large amplitude vibrations. For an overview of these theoretical approaches we refer to ref. [44]. Some remarks can be made:

- 1) All methods satisfying the required criteria are DFT based methods. It must be noted however that we used only pure methods in the sense that the same level of theory is used to calculate, for example, geometries and frequencies. Several literature works use so called combined methods, where the geometries are calculated, for example, at the B3LYP/6-31G(d) level and the energies are refined at the QCISD/6-31G(d) level. For relevant references we refer to refs. [9v,46,47] and references therein. The latter methods have proven to be accurate for calculating reaction barriers of similar addition reactions.^[9v] However they cannot be retained for radical polymerization reactions in which larger alkyl radicals, that is, up to 30 carbon atoms are involved, since the computational cost would not be feasible. Within this light DFT based methods are cost-effective alternatives for the study of larger systems.
- 2) Some pure DFT methods, such as BP86 and BLYP can be retained for some of the addition reactions but they cannot

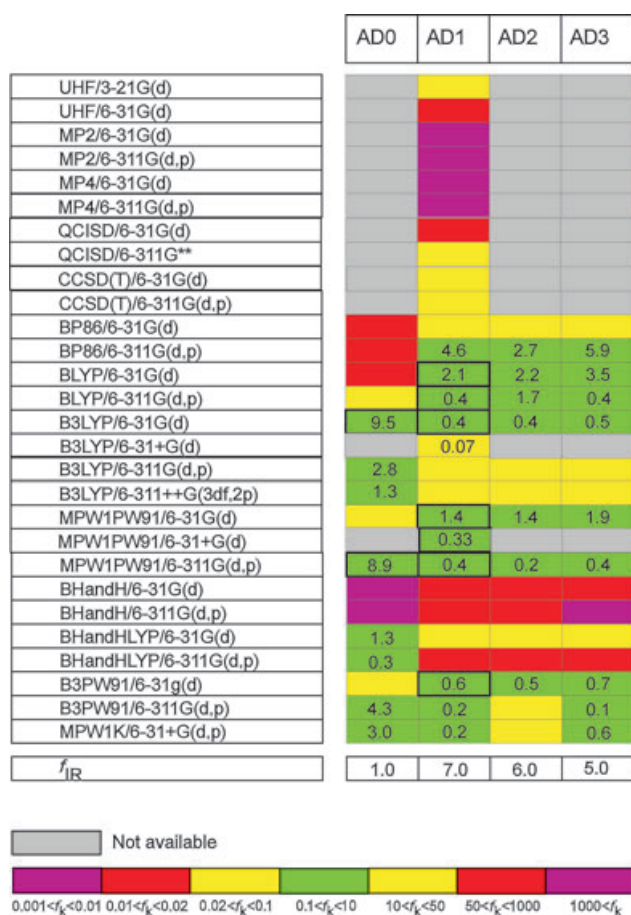


Figure 3. Schematic overview of the error analysis on the reactions AD0, AD1, AD2 and AD3. The numbers indicated in the green boxes represent $\langle f_k \rangle$ in the temperature range 300–600 K. The green boxes with an additional black border indicate levels of theory that fulfill both Criteria I and II. Criterion I is only applied to AD0 and AD1.

be proposed as a suitable theoretical scheme for all studied reactions. The BP86/6-311G(d,p) and BLYP methods fulfill criterion II for reactions AD1, AD2 and AD3 but still give errors on the rate coefficient that are larger than some of the hybrid functionals.

- Only some hybrid density functional methods give the satisfactory results for all reactions, namely B3LYP, MPW1PW91 and B3PW91. For these functionals the double zeta basis set with single d-type polarization functions—generally known as 6-31G(d)—gives the smallest errors with respect to the experimental data. The introduction of some exact Hartree–Fock exchange into the functional has a profound influence on the kinetic results.
- For the additions AD1, AD2 and AD3, internal rotations enhance the rate constant, since for these reactions additional transition states come into play and thus more reaction pathways can be assessed. This increment implies that some methods that already overestimate the experimental rate constant ($f_k > 1$) [such as BP86/6-311G(d,p) or BLYP/6-31G(d)] do not fulfill criterion II anymore when accounting for internal rotations.

For completeness, we also give the reaction barriers at 0 K for the various levels of theory in Table 2. When increasing the basis set from 6-31G(d) to 6-311G(d,p) the reaction barriers increase by ≈ 2 –6 kJ mol⁻¹ depending on the functional used. An important fraction of these effects is caused by a change in

Table 2. ΔE_0 [kJ mol⁻¹] for ADn at various levels of theory

HF/post-HF	basis set	TSAD0	TSAD1	TSAD2	TSAD3
UHF	3-21G(d)		35.76		
UHF	6-31G(d)		48.30		
MP2	6-31G(d)		66.67		
MP2	6-311G(d,p)		62.62		
MP4	6-31G(d)		62.64		
MP4	6-311G(d,p) ^[a]		54.71		
qcisd	6-31G(d)		44.54		
qcisd	6-311G(d,p)		41.17		
ccsd(T)	6-31G(d)		41.64		
ccsd(T)	6-311G(d,p) ^[a]		35.88		
DFT	basis set				
BP86	6-31G(d)	17.36	18.95	17.47	17.60
BP86	6-311G(d,p)	19.90	22.38	21.51	21.56
BLYP	6-31G(d)	22.10	24.59	23.05	23.16
BLYP	6-311G(d,p)	25.47	30.05	29.23	29.25
B3LYP	6-31G(d)	27.82	29.70	28.12	28.25
B3LYP	6-311G(d,p)	32.05	34.89	33.90	33.94
B3LYP	6-311++G(3df,2p)	35.06	38.20	37.31	37.19
MPW1PW91	6-31G(d)	24.72	25.51	24.02	24.17
MPW1PW91	6-311G(d,p)	28.12	29.33	25.71	28.37
BHandH	6-31G(d)	9.31	7.66	5.80	5.97
BHandH	6-311G(d,p)	12.97	11.62	10.08	10.31
BHandHLYP	6-31G(d)	34.60	35.67	34.10	34.21
BHandHLYP	6-311G(d,p)	39.63	41.30	40.11	40.18
B3PW91	6-31G(d)	27.59	29.07	27.60	27.73
B3PW91	6-311G(d,p)	30.85	32.83	32.29	31.95
MPW1K	6-31+G(d)	31.97	32.43	31.03	31.20

[a] Geometries and frequencies were taken from the B3LYP/6-31G(d) level, while the energies were calculated at the current level.

the basis set superposition error (BSSE) for the forming bond.^[46] The large BSSE for the 6-31G(d) basis artificially lowers the electronic energy of the transition state relative to the energy of the reactants and lowers the product energy even more. An enlargement of the basis set size decreases the BSSE and thus shifts up the relative energies, thereby increasing the radical addition barrier. Similar effects were seen by Saeys et al. and Barone et al. on radical addition reactions.^[9v,r]

3. Conclusions

Herein, we studied additions of carbon-centered radicals to ethene, which are important for free-radical polymerizations leading to polyethylene (PE). The principal aim was to derive a cost-effective method for calculating the rate constant for this prototype of reactions. Cost-effectiveness is defined in the sense that the method must be accurate but also computationally feasible for additions in which longer alkyl radicals are involved. The selection is based on the direct comparison of theoretical and experimental rate constants in the temperature

range 300 to 600 K. Various Hartree–Fock, post-Hartree–Fock and DFT methods were investigated. The comparative study learned that some hybrid DFT methods, that is, B3LYP, MPW1PW91 and B3PW91, in combination with double zeta basis sets, that is, 6-31G(d), gave the best results for all radical addition reactions. The theoretical rate constants deviate at maximum by a factor of two with respect to the experimental data in the whole temperature range. The selected methods deviate at maximum by 3 kJ mol⁻¹ with the experimental slope in the whole temperature range, at least for the reactions where the experimental data are accurate enough to use criterion I, that is, AD1 and AD0. Anyway for all considered reactions the theoretical rate constant and experimental one deviate not more than a factor ten in the temperature interval from 300 to 600 K. We have also given an indication of the possible influence of taking into account internal rotations on the final results for the rate constant. For the AD1, AD2 and AD3 reactions this extension leads to an enhancement of the reaction rate by about a factor five. Anyway the influence of internal rotations was not the determining factor for selecting appropriate levels of theory. Despite the good correspondence of the selected methods with the experimental data for the four considered additions, we do not claim that these methods are the best methods for all possible addition reactions to olefins. For elaborate discussions we refer to the work of Radom and co-workers.^[29,30] But within the scope of PE polymerizations the selected DFT methods provide a viable alternative due to their accuracy and their scalability to larger systems.

Acknowledgments

This work is supported by the Fund for Scientific Research–Flanders (FWO) and the Research Board of Ghent University.

Keywords: ab initio calculations · density functional calculations · kinetics · polymerization · radical reactions

- [1] M. Buback, R. G. Gilbert, R. A. Hutchinson, B. Klumperman, F. D. Kuchta, B. G. Manders, K. F. O'Driscoll, G. T. Russell, J. Schweer, *J. Macromol. Sci. Phys.* **1995**, *196*, 3267–3280.
- [2] T. P. Davis, K. F. O'Driscoll, M. C. Piton, M. A. Winnik, *Polym. Int.* **1991**, *24*, 65–70.
- [3] S. Beuermann, M. Buback, *Prog. Polym. Sci.* **2002**, *27*, 191–254.
- [4] a) D. L. Baulch, C. J. Cobos, R. A. Cox, C. Esser, P. Frank, Th. Just, J. A. Kerr, M. J. Pilling, J. Troe, R. W. Walker, J. Warnatz, *J. Phys. Chem. Ref. Data* **1992**, *21*, 411–429; b) W. Tsang, R. F. Hampson, *J. Phys. Chem. Ref. Data* **1986**, *15*, 1087; c) P. M. Holt, J. A. Kerr, *Int. J. Chem. Kinet.* **1977**, *9*, 185; d) P. Camilleri, R. M. Marschall, H. Purnell, *J. Chem. Soc. Faraday Trans. 1* **1975**, *71*, 1491; e) J. A. Kerr, M. J. Parsonage, *Evaluated kinetic data on gas phase addition reactions. Reactions of atoms and radicals with alkenes, alkynes and aromatic compounds*, Butterworths, London, **1972**; f) A. M. Hogg, P. Kebarle, *J. Am. Chem. Soc.* **1964**, *86*, 4558–4562
- [5] a) V. D. Knyazev, I. R. Slagle, *J. Phys. Chem.* **1996**, *100*, 5318–5328; b) K. W. Watkins, L. A. O'Deen, *J. Phys. Chem.* **1969**, *73*, 4094–4102; d) W. E. Morganroth, J. G. Calvert, *J. Am. Chem. Soc.* **1966**, *88*, 5387; e) J. A. Kerr, A. F. Trotman-Dickenson, *J. Chem. Soc.* **1960**, 1611.
- [6] a) K. W. Watkins, D. R. Lawson, *J. Phys. Chem.* **1971**, *75*, 1632; b) J. A. Kerr, A. F. Trotman-Dickenson, *Trans. Faraday Soc.* **1959**, *55*, 572.
- [7] a) K. W. Watkins, L. A. O'Deen, *J. Phys. Chem.* **1969**, *73*, 4094–4102; b) J. A. Kerr, A. F. Trotman-Dickenson, *J. Chem. Soc.* **1960**, 1602.
- [8] M. Buback, J. Schweer, *Z. Phys. Chem., Abt. B* **1989**, *161*, 153–165.
- [9] a) K. N. Houk, M. N. Paddon-Row, D. C. Spellmeyer, N. G. Rondan, S. Nagase, *J. Org. Chem.* **1986**, *51*, 2874; b) R. Arnaud, R. Subra, V. Barone, F. Lelj, S. Olivella, A. Sole, N. Russo, *J. Chem. Soc. Perkin Trans. 2* **1986**, 1517; c) T. Clark, *J. Chem. Soc. Chem. Commun.* **1986**, 1774; d) T. Fueno, M. Kamachi, *Macromolecules* **1988**, *21*, 908; e) C. Gonzales, C. Sosa, H. B. Schlegel, *J. Phys. Chem.* **1989**, *93*, 2435; f) C. Gonzales, C. Sosa, H. B. Schlegel *J. Phys. Chem.* **1989**, *93*, 8388; g) R. Arnaud, *New J. Chem.*, **1989**, *13*, 543; h) H. Zipse, J. He, K. N. Houk, B. J. Giese, *J. Am. Chem. Soc.* **1991**, *113*, 4324; i) R. Arnaud, S. Vidal, *New J. Chem.* **1992**, *16*, 471; j) D. J. Tozer, J. S. Andrews, R. D. Amos, N. C. Handy, *Chem. Phys. Lett.* **1992**, *199*, 229; k) C. Schmidt, M. Warken, N. C. Handy, *Chem. Phys. Lett.* **1993**, *211*, 272; l) M. W. Wong, A. Pross, L. Radom, *J. Am. Chem. Soc.* **1993**, *115*, 11050; m) M. W. Wong, A. Pross, L. Radom, *Isr. J. Chem.* **1993**, *33*, 415; n) T. P. Davis, S. C. Rogers, *Macromol. Theory Simul.* **1994**, *3*, 905; o) M. W. Wong, A. Pross, L. Radom, *J. Am. Chem. Soc.* **1994**, *116*, 6284; p) M. W. Wong, A. Pross, L. Radom, *J. Am. Chem. Soc.* **1994**, *116*, 11938; q) J. Espinosa-Garcia, J. C. Corchado, G. Leroy, *J. Phys. Chem.* **1995**, *99*, 13926; r) V. Barone, L. Orlandini, *Chem. Phys. Lett.* **1995**, *246*, 45; s) R. Gomez-Balderas, M. L. Coote, D. J. Henry, H. Fischer, L. Radom, *J. Phys. Chem. A* **2003**, *107*, 6082; t) D. J. Henry, M. L. Coote, R. Gomez-Balderas, L. Radom *J. Am. Chem. Soc.* **2004**, *126*, 1732–1740; u) M. Saeys, M. F. Reyniers, G. B. Marin, V. Van Speybroeck, M. Waroquier, *J. Phys. Chem. A* **2003**, *107*, 9147; v) M. Saeys, M. F. Reyniers, G. B. Marin, V. Van Speybroeck, M. Waroquier, *AIChE J.* **2004**, *50*, 426;
- [10] H. Fischer, L. Radom, *Angew. Chem.* **2001**, *113*, 1380–1414; *Angew. Chem. Int. Ed.* **2001**, *40*, 1340–1371.
- [11] J. P. A. Heuts, R. G. Gilbert, L. Radom, *Macromolecules* **1995**, *28*, 8771–8781.
- [12] J. P. A. Heuts, R. G. Gilbert, L. Radom, *J. Phys. Chem.* **1996**, *100*, 18997–19006.
- [13] H. Eyring, *J. Chem. Phys.* **1935**, *3*, 107; A more comprehensive treatment can be found in W. F. K. Wynne-Jones, H. Eyring, *J. Chem. Phys.* **1935**, *3*, 492; This article is reproduced in full in M. H. Back, K. L. Laidler, *Selected readings in chemical kinetics*, Pergamon, Oxford, **1967**.
- [14] a) M. G. Evans, M. Polanyi, *Trans. Faraday Soc.* **1935**, *31*, 875; b) M. G. Evans, M. Polanyi, *Trans. Faraday Soc.* **1937**, *33*, 448.
- [15] K. J. Laidler, *Chemical kinetics*, HarperCollins Publishers Inc., New York, **1987**.
- [16] D. A. Mc. Quarrie, J. D. Simon, *Physical Chemistry—A molecular approach*, University Science Books, Sausalito, California, **1997**.
- [17] For reviews, see, for example, a) P. Pechukas in *Dynamics of Molecular Collisions, Part B* (Ed.: W. H. Miller), Plenum Press, New York, **1976**; b) K. J. Laidler, M. C. King, *J. Phys. Chem.* **1983**, *87*, 2657; c) D. G. Truhlar, W. L. Hase, J. T. Hynes, *J. Phys. Chem.* **1983**, *87*, 2664; d) R. G. Gilbert, S. C. Smith, *Theory of Unimolecular and Recombination Reactions*, Blackwell, Oxford, **1990**.
- [18] a) H. F. Schaefer, III in *Atom-Molecule Collision Theory* (Ed.: R. B. Bernstein), Plenum, New York, **1979**, p. 45; b) C. Sosa, C.; H. B. Schlegel, *Int. J. Quantum Chem.* **1986**, *29*, 1001; c) C. Sosa, H. B. Schlegel, *Int. J. Quantum Chem. Symp.* **1987**, *21*, 267; d) C. Gonzalez, C. Sosa, H. B. Schlegel, *J. Phys. Chem.* **1989**, *93*, 2435.
- [19] a) C. Moller, M. S. Plesset, *Phys. Rev.* **1934**, *46*, 618; b) J. A. Pople, R. Krishnan, R. Seeger, *Int. J. Quantum Chem. Symp.* **1976**, *10*, 1, and references therein; c) R. Krishnan, M. J. Frisch, J. A. Pople, *J. Chem. Phys.* **1980**, *72*, 4244.
- [20] a) H. B. Schlegel, *J. Chem. Phys.* **1986**, *84*, 4530; b) H. B. Schlegel, *J. Phys. Chem.* **1988**, *92*, 3075; c) W. Chen, H. B. Schlegel, *J. Chem. Phys.* **1994**, *101*, 5957.
- [21] a) H.-J. Werner, *Adv. Chem. Phys.* **1987**, *49*, 1; b) R. Shepard, *Adv. Chem. Phys.* **1987**, *49*, 63.
- [22] An example of a reference work: R. G. Parr, W. Yang, *Density-Functional Theory of Atoms and Molecules*, Oxford University Press, New York, **1989**.
- [23] B. J. Lynch, D. G. Truhlar, *J. Phys. Chem. A* **2001**, *105*, 2936.
- [24] G. Katzer, A. F. Sax, *J. Phys. Chem. A* **2002**, *106*, 7204–7215.
- [25] a) S. Mizushima, *Structure of Molecules and Internal Rotation*, Academic, New York, **1954**; b) W. J. Orville-Thomas, *Internal rotation in molecules*, Wiley, London, **1974**; c) D. G. Lister, J. N. MacDonald and N. L. Owen, *Internal rotation and Inversion*, Academic, London, **1978**.

- [26] a) E. B. Wilson, *Adv. Chem. Phys.* **1959**, *2*, 367; b) J. P. Lowe, *Prog. Phys. Org. Chem.* **1968**, *6*, 1; c) D. A. Long, *J. Mol. Struct.* **1985**, *126*, 9; d) U. Berg, J. Sandström, *Adv. Phys. Org. Chem.* **1989**, *25*, 1.
- [27] V. Van Speybroeck, D. Van Neck, M. Waroquier, S. Wauters, M. Saeys, G. B. Marin, *J. Phys. Chem. A* **2000**, *104*, 10939–10950.
- [28] J. A. Pople, R. K. Nesbet, *J. Chem. Phys.* **1954**, *22*, 571.
- [29] R. Gomez-Balderas, M. L. Coote, D. J. Henry, H. Fischer, L. Radom, *J. Phys. Chem. A* **2004**, *108*, 2874–2883.
- [30] M. L. Coote, G. P. F. Wood, L. Radom, *J. Phys. Chem. A* **2002**, *106*, 12124–12138.
- [31] Gaussian98 (Revision A.7), M. J. Frisch, G. W. Trucks, H. B. Schlegel, G. E. Scuseria, M. A. Robb, J. R. Cheeseman, V. G. Zakrzewski, J. A. Montgomery, R. E. Stratmann, J. C. Burant, S. Dapprich, J. M. Millam, A. D. Daniels, K. N. Kudin, M. C. Strain, O. Farkas, J. Tomasi, V. Barone, M. Cossi, R. Cammi, B. Mennucci, C. Pomelli, C. Adamo, S. Clifford, J. Ochterski, G. A. Petersson, P. Y. Ayala, Q. Cui, K. Morokuma, D. K. Malick, A. D. Rabuck, K. Raghavachari, J. B. Foresman, J. Cioslowski, J. V. Ortiz, B. B. Stefanov, G. Liu, A. Liashenko, P. Piskorz, I. Komaromi, R. Gomperts, R. L. Martin, D. J. Fox, T. Keith, M. A. Al-Laham, C. Y. Peng, A. Nanayakkara, C. Gonzalez, M. Challacombe, P. M. W. Gill, B. G. Johnson, W. Chen, M. W. Wong, J. L. Andres, M. Head-Gordon, E. S. Replogle, J. A. Pople, Gaussian, Inc., Pittsburgh, PA, **1998**.
- [32] J. A. Pople, M. Head-Gordon, K. Raghavachari, *J. Chem. Phys.* **1987**, *87*, 5968.
- [33] a) G. D. Purvis, III, R. J. Bartlett, *J. Chem. Phys.* **1982**, *76*, 1910; b) G. E. Scuseria, C. L. Janssen, H. F. Schaefer, III, *J. Chem. Phys.* **1989**, *89*, 7392; c) G. E. Scuseria, H. F. Schaefer, III, *J. Chem. Phys.* **1989**, *90*, 3700.
- [34] A. D. Becke, *Phys. Rev. A* **1988**, *38*, 3098.
- [35] a) K. Burke, J. P. Perdew, Y. Wang in *Electronic Density Functional Theory: Recent Progress and New Directions* (Eds.: J. F. Dobson, G. Vignale, M. P. Das), Plenum Press, New York, **1998**; b) J. P. Perdew in *Electronic Structure of Solids '91* (Eds.: P. Ziesche, H. Eschrig), Akademie Verlag, Berlin, **1991**, p. 11; c) J. P. Perdew, J. A. Chevary, S. H. Vosko, K. A. Jackson, M. R. Pederson, D. J. Singh, C. Fiolhais, *Phys. Rev. B* **1992**, *46*, 6671; d) J. P. Perdew, J. A. Chevary, S. H. Vosko, K. A. Jackson, M. R. Pederson, D. J. Singh, C. Fiolhais, *Phys. Rev. B* **1993**, *48*, 4978; e) J. P. Perdew, K. Burke, Y. Wang, *Phys. Rev. B* **1996**, *54*, 16533.
- [36] a) C. Lee, W. Wang, R. G. Parr, *Phys. Rev. B* **1988**, *37*, 785; b) B. Miehlich, A. Savin, H. Stoll, H. Preuss, *Chem. Phys. Lett.* **1989**, *157*, 200.
- [37] D. Becke, *J. Chem. Phys.* **1993**, *98*, 5648.
- [38] Adamo, V. Barone, *J. Chem. Phys.* **1998**, *108*, 664.
- [39] a) B. J. Lynch, D. G. Truhlar, *J. Phys. Chem. A* **2001**, *105*, 2936; b) A. P. Scott, L. Radom, *J. Phys. Chem.* **1996**, *100*, 16502–16513.
- [40] The functionals are defined according to the definition given in the Gaussian manual.
- [41] B. J. Lynch, P. L. Fast, M. Harris, D. G. Truhlar, *J. Phys. Chem. A* **2000**, *104*, 4811.
- [42] B. J. Lynch, Y. Zhao, D. G. Truhlar, *J. Phys. Chem. A* **2003**, *107*, 1384.
- [43] P. Vansteenkiste, V. Van Speybroeck, G. B. Marin, M. Waroquier, *J. Phys. Chem. A* **2003**, *107*, 3139.
- [44] V. Van Speybroeck, P. Vansteenkiste, D. Van Neck, M. Waroquier, unpublished results.
- [45] V. Barone, *J. Chem. Phys.* **2004**, *120*, 3059.
- [46] M. W. Wong, L. Radom, *J. Phys. Chem. A* **1998**, *102*, 2237.
- [47] Y.-Y. Chuang, E. L. Coitino, D. G. Truhlar, *J. Phys. Chem. A* **2000**, *104*, 446.
- [48] F. B. van Duijneveldt, J. G. C. M. van Duijneveldt-van de Rijdt, J. H. van-Lenthe, *Chem. Rev.* **1994**, *94*, 1873.

Received: June 11, 2004

Early View Article
Published online on December 9, 2004